Lithography, Plasmonics and Sub-wavelength Aperture Exposure Technology

Yves Ngu[1*], Marty Peckerar[1], Xiaoping Liu[1], Mario Dagenais[1], Mike Messina[2] and Jon Barry[1]
[1]Dept. of Electrical and Computer Engineering, University of Maryland, College Park, MD 20742
[2]ASML, Honolulu, HI 96813

1. Introduction

The subwavelength transmission phenomenon has recently received significant attention in the theoretical physics community. Light incident on a metal thin film establishes oscillation in the mobile charge density (ripples in the "Fermi sea".) These ripples, in turn, excite cavity modes in circular apertures in the thin film. These cavity modes acts as intense light sources, drawing energy from their surroundings on which light is incident. The net transmission is far greater than the aperture area alone would dictate. In this article we examine the incorporation of this technique in photolithographic mask design to provide inexpensive methods for performing ultra-high resolution photolithographic systems. We describe the ion-beam fabrication of an optical proximity corrected (OPC) phase-mask mask with significantly reduced "fill-factor" over those masks manufactured using current direct-write technologies. The approach fuses two principles: π-phase shifting and sub-wavelength aperture transmission (SWAT).

2. Mask Design and Experimental Projection Lithography Results

Rather than creating a mask with continuous clearand opaque regions, as shown in Fig. 1 (a), a square "dot matrix" mask structure is created on a 100 nm thick silver film as in Fig 1 (b). The mask is created by a collection of extremely fine array of dots written on a 6" x 6 " glass plate using a focused- ion-beam (fib). The hole diameter is about 200 nm. The π-phase shifting was accomplished by creating, around the main pattern, a ring of dots whose clear substrates have been over-etched to change the optical path length by π-radians as illustrated in Fig. 1 (c). While the pattern intensity is the same (just the square of the amplitude, a real, signless number), the amplitudes sum was expected to create an extremely high optical contrast.

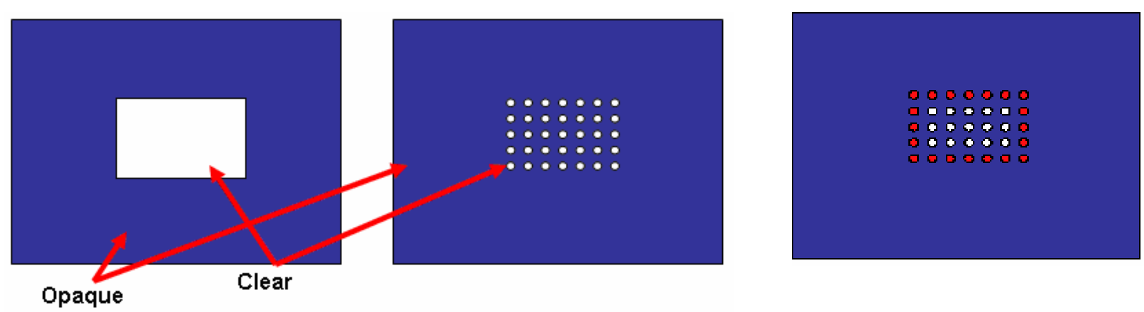

(a) (b) (c)

Figure 1: (a) A conventional chrome photoplate; (b) a "sub-wavelength" photoplate; (c) a "sub-wavelength" photoplate with over-etched outer ring

The mask fabricated was geared towards examining the effect of hole spacing, hole depth as well as the influence of correctional holes. The different characteristics of the mask are the following:

- Three hole spacing (d1=0.5um and d2=0.3um and d3=0.7um) arranged in four array patterns (shown in Fig. 2)
- The four array patterns are:
    - Inner: 1st inner row and column "over etched"
    - Outer: outer row and column "over etched"
    - Normal: simple 10x10 array
    - Star: simple 10x10 array + one extra hole at each corner (for corner correction)

- Short milling: 30 sec milling of 10x10box (+ 30 sec milling of "over etched" rows and column ie. Inner and outer) AND 30sec milling of Star pattern
- Long milling: 1 min. milling of 10x10box (+ 30 sec milling of "over etched" rows and column ie. Inner and outer) AND 1 min. milling of Star pattern

The various patterns of Fig. 2 are then stepped over the mask while varying the whole spacing (d1-3), the hole depth (via short and long milling).

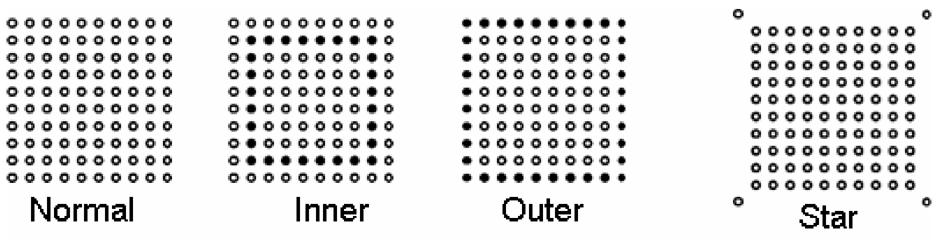

Figure 2: Array patterns; hole spacing is center to center

The mask was then used to expose the photoresist on a silicon wafer. The exposure was via 4X projection printing. The exposure was done at various focuses and intensities. For each hole spacing arrangement, the array of holes formed a square with the following equation describing the linear dimension T of the square array

$$T = 9 * d + D \quad ,$$

where d represents the hole spacing and D is the diameter of the holes (about 200 nm). For 300nm hole spacing, the array size was 2.9 µm with an expected 4X projected pattern of 0.75 µm. The SEM images of a resolved *Normal* and *Star* pattern with 300nm hole spacing are shown in Fig. 3. The patterns resolved as squares with rounded corners. Dimensions of the resolved patterns were estimated from their SEM images. The resolved patterns were larger than the anticipated. The pattern size obtained from *normal* or *star* patterns were very similar to each other and adding the extra holes at the edge of the patterns did not correct the small roundness of the images. The smallest exposed patterns were obtained from *Normal* patterns. Other optically corrected patterns (*Inner* or *Outer* patterns) resulted in larger patterns.

(a) (b)

Figure 3: SEM image of resolved pattern with X and Y measurement; a) pattern 19; b) pattern 24

3. Conclusion

The observed enhanced transmission through the 300 nm spacing hole arrays and its spacing dependence appears to be a plasmonic effect. The existence of a collective effect of the various holes explains the similar transmission behavior of the 'normal' and 'star' pattern. Further measurements, including a study of the polarization dependence of the transmission and different focusing geometries, are in progress. Since the number of addressed pixels is far less than the number of pixels in typical exposure patterns for focused-ion-beam and electron-beam writing, our results point toward an exciting potential applications that would appreciably reduce the writing times of these systems in high resolution applications.